



Published in final edited form as:

Circ Res. 2017 July 07; 121(2): 125–136. doi:10.1161/CIRCRESAHA.117.311094.

Role of STIM1 in Hypertrophy-Related Contractile Dysfunction

Constantine D. Troupes¹, Markus Wallner¹, Giulia Borghetti¹, Chen Zhang¹, Sadia Mohsin¹, Dirk von Lewinski², Remus M. Berretta¹, Hajime Kubo¹, Xiongwen Chen¹, Jonathan Soboloff³, and Steven Houser¹

¹Cardiovascular Research Center; Lewis Katz School of Medicine; Temple University; Philadelphia, PA, 19140, USA

²Department of Cardiology, Medical University of Graz, Auenbruggerplatz 15, 8036 Graz, Austria

³Fels Institute for Cancer Research and Molecular Biology; Lewis Katz School of Medicine; Temple University School of Medicine; Philadelphia, PA 19140, USA

Abstract

Rationale—Pathological increases in cardiac afterload result in myocyte hypertrophy with changes in myocyte electrical and mechanical phenotype. Remodeling of contractile and signaling Ca^{2+} occurs in pathological hypertrophy and is central to myocyte remodeling. Stromal Interaction Molecule 1 (STIM1) regulates Ca^{2+} signaling in many cell types by sensing low endoplasmic reticular Ca^{2+} levels and then coupling to plasma membrane Orai channels to induce a Ca^{2+} influx pathway. Previous reports suggest that STIM1 may play a role in cardiac hypertrophy but its role in electrical and mechanical phenotypic alterations are not well understood.

Objective—To define the contributions of STIM1-mediated Ca^{2+} influx on electrical and mechanical properties of normal and diseased myocytes, and to determine if Orai channels are obligatory partners for STIM1 in these processes using a clinically relevant large animal model of hypertrophy.

Methods and Results—Cardiac hypertrophy was induced by slow progressive pressure overload in adult cats. Hypertrophied myocytes had increased STIM1 expression and activity, which correlated with altered Ca^{2+} handling and action potential (AP) prolongation. Exposure of hypertrophied myocytes to the Orai channel blocker BTP2 caused in a reduction of AP duration and reduced diastolic Ca^{2+} spark rate. BTP2 had no effect on normal myocytes. Forced expression of STIM1 in cultured adult feline ventricular myocytes increased diastolic spark rate and prolonged AP duration. STIM1 expression produced an increase in the amount of Ca^{2+} stored within the sarcoplasmic reticulum and activated Ca^{2+} /calmodulin-dependent protein kinase II. STIM1 expression also increased spark rates and induced spontaneous APs. STIM1 effects were eliminated by either BTP2 or by co-expression of a dominant negative Orai construct.

Address correspondence to: Dr. Steven R. Houser, Lewis Katz School of Medicine, Temple University, Cardiovascular Research Center, 3500 N. Broad St. MERB 1080C, Philadelphia, PA 19140, Phone: 215-707-3278, Fax: 215-707-0170, srhouser@temple.edu.

DISCLOSURES

None

Conclusions—STIM1 can associate with Orai in cardiac myocytes to produce a Ca^{2+} influx pathway that can prolong the AP duration and load the SR and likely contributes to the altered electromechanical properties of the hypertrophied heart.

Keywords

calcium; cardiac myocyte hypertrophy; cardiac dysfunction; cardiac myocytes; STIM1

Subject Terms

Animal Models of Human Disease; Calcium Cycling/Excitation-Contraction Coupling; Hypertrophy; Ion Channels/Membrane Transport

INTRODUCTION

Cardiovascular diseases such as hypertension, valvular disease and myocardial infarction-induced ventricular dilation all impose a persistent, pathological increase in the work demands (afterload) of the heart¹⁻³. Neurohumoral systems are activated to increase the contractile $[\text{Ca}^{2+}]$ required to support the enhanced contractile demands of the diseased heart⁴. Over time, the persistently overworked left ventricle remodels, increasing wall thickness to at least partially compensate for increased wall stress⁵. This hypertrophy occurs at both the organ and cellular level, with an increase in left ventricular mass and an increase in cardiac myocyte size⁶. The signaling processes that produce pathological myocyte hypertrophy have essential Ca^{2+} -dependent signaling steps, but there is some evidence that the sources of Ca^{2+} for enhanced contractile function and for hypertrophic signaling are distinct⁷⁻⁹.

Hypertrophied myocytes adopt a modified electromechanical phenotype. The action potential (AP) is prolonged, Ca^{2+} transients are disrupted with slower kinetics, sarcoplasmic reticulum (SR) Ca^{2+} reuptake is slowed, Ca^{2+} leak from the SR is increased to reduce SR Ca^{2+} stores, and these systems become unresponsive to sympathetic regulation, reducing contractility reserve^{10, 11}. Alterations in Ca^{2+} regulation in hypertrophy is also linked to increased risk of arrhythmias and HF^{12, 13}. Indeed, left ventricular hypertrophy (LVH) is an independent predictor of hospitalization and sudden cardiac death^{14, 15}.

The molecular bases of altered contractile and hypertrophic signaling $[\text{Ca}^{2+}]$ are still not fully understood and are the topic of this study⁷. Here, we specifically study the role of the SR protein, Stromal Interaction Molecule 1 (STIM1), and its sarcolemmal partner protein Orai in the development of electrical and contractile remodeling of adult ventricular myocytes after pressure overload. There is some evidence from previous reports that these proteins are present in cardiac myocytes and their abundance increases in disease states^{16, 17}. This increase has been linked to maladaptive cardiac hypertrophy^{18, 19}. However, the consequence of STIM-mediated Ca^{2+} influx on the function of hypertrophied cardiac myocytes are not clearly defined, especially in large animals with Ca^{2+} regulation similar to the human heart. In this study, we explore the idea that alterations in the electrical and mechanical properties of the hypertrophied heart involves STIM-dependent Ca^{2+} entry and blocking this influx pathway can improve these disturbances.

STIM and Orai proteins are widely known as the key mediators of store operated Ca^{2+} entry (SOCE), a nearly ubiquitous process in non-excitable cells^{20, 21}. In mammals, there are two isoforms of STIM (STIM1 and STIM2) that are present in the endoplasmic reticulum (ER)²², and three homologs of Orai (Orai1, Orai2 and Orai3) located on the plasma membrane. SOCE occurs during periods of ER Ca^{2+} depletion, which can physiologically occur after inositol triphosphate receptor activation of ER Ca^{2+} release. STIM senses reduced ER $[\text{Ca}^{2+}]$ via a luminal EF hand motif and subsequently undergoes a conformational change resulting in oligomerization²³. Activated STIM proteins are then able to bind and gate Orai channels located in the plasma membrane, which are highly selective, low conductance Ca^{2+} channels²⁴. The resulting Ca^{2+} influx adds Ca^{2+} to the ER and is also thought to activate Ca^{2+} dependent signaling processes²⁵.

Cardiac myocytes have robust Ca^{2+} entry through the L-type Ca^{2+} channel with each heartbeat. This Ca^{2+} influx induces Ca^{2+} release from the SR to initiate contraction and also provides Ca^{2+} to load the SR²⁶. The SR releases and takes up Ca^{2+} with each heartbeat and is never depleted during normal physiological function. It is therefore not surprising that a physiological role for STIM and Orai in cardiac myocytes has not been defined. Yet, many independent groups have found STIM1 to be present in cardiac myocytes²⁷, though there are conflicting reports on the function of STIM1 and SOCE in these cells^{16, 28, 29}. In the diseased heart, SR Ca^{2+} regulation is altered¹¹ and increased SOCE activity has been observed in rodent cardiac disease models. Some groups have linked this increased activity with pathological hypertrophy. A recent study¹⁶ suggested that activated STIM1 can increase SR Ca^{2+} loading by binding to phospholamban (PLB) and thereby regulating SERCA activity. This function of STIM1 in normal myocytes was found to be independent of Orai and SOCE. Collectively, these reports suggest that Ca^{2+} influx through STIM and Orai proteins might be involved in the abnormal Ca^{2+} regulation found in diseased ventricular myocytes. However, this hypothesis has not been tested in a clinically relevant large animal model.

The objective of our study was to explore the if/how STIM1 contributes to the changes in electrical and contractile phenotype of hypertrophied ventricular myocytes from the adult feline heart. We used the feline model because, unlike rodent models, it has electrical and Ca^{2+} regulatory properties that are similar to those of human^{30, 31}. Our experiments tested the hypothesis that in myocytes with hypertrophy from persistent pressure overload, SR based STIM1 is activated and partners with surface membrane Orai to produce Ca^{2+} entry that contributes to their altered phenotype. Our results support the idea that STIM1 and Orai are expressed, but do not contribute to the electromechanical function of the healthy heart. In hypertrophied myocytes, STIM1 becomes activated and induces Ca^{2+} entry after associating with Orai, resulting in enhanced SR loading and AP prolongation. Excessive STIM1-mediated Ca^{2+} entry caused Ca^{2+} sparks, spontaneous APs, and cell death. These results suggest that STIM1 activation in disease might help preserve SR Ca^{2+} load but predisposes myocytes to arrhythmias and death.

METHODS

Methods are described in detail in the online data supplement. Briefly, LVH was induced in young cats by aortic banding, and myocytes were isolated using collagenase as described in detail previously. After isolation, Ca²⁺ transients, Ca²⁺ currents, Ca²⁺ sparks and cell shortening were measured using standard techniques described in detail in previous reports from our group^{28, 32}. Isolated myocytes from control and banded animals were exposed to 1 μmol/L BTP2 (*N*-[4-[3,5-*Bis*(trifluoromethyl)-1*H*-pyrazol-1-yl]phenyl]-4-methyl-1,2,3-thiadiazole-5-carboxamide), *in vitro*, in cell physiology experiments. Myocytes were also studied in primary culture and infected with adenovirus overnight, as described previously³³. Experiments with these myocytes were completed within 36 hours of isolation to minimize effects of culture-dependent phenotypic “drift”^{34, 35}.

RESULTS

Pressure overload hypertrophy is associated with increased STIM1 expression and activity

Slow progressive pressure overload was induced by aortic banding of young animals, to induce LVH, similar to our previous reports^{36, 37}. This procedure caused significant increases in systolic proximal aortic pressure after 4 months (proximal vs distal pressure: 149.8±15.3 vs 87±9.6 mmHg, Figure 1A) and a systolic pressure gradient of 63 mmHg across the aortic constriction. There are no significant decreases in ECHO-derived systolic function in this model (Figure 1B). End-diastolic wall thickness was significantly increased by banding as measured by echocardiography (Banded vs Sham: 7.5±0.5 vs 4.6±0.3 mm, *p* 0.05, Figure 1C). The heart weight to body weight (HW/BW) ratio was significantly increased in banded versus sham animals (9.2±1.13 vs 4.6±0.4, *p* 0.01, Figure 1D)

Pressure overload was associated with increases in the expression of SOCE-related mRNA. Real time polymerase chain reaction (RT-PCR) was used to measure mRNA levels of SOCE proteins in mRNA from isolated myocytes. Myocytes from banded animals had significantly greater amounts of STIM1 and Orai3 mRNA, and non-significant increases in STIM2 and Orai1 mRNA (Figure 1E). Orai2 was not detected in normal or hypertrophied feline myocytes.

Immunofluorescence staining of isolated myocytes showed that STIM1 exhibited a striated fashion in control myocytes (Figure 1F, top), with what appeared to be uniform intensity along the striations. Co-staining with actinin suggests that STIM1 is localized near the Z-line, where the sarcolemma/SR dyad resides (Online Figure I, A). This staining pattern is similar to that seen by others¹⁶. Hypertrophied myocytes from banded animals exhibited a more uneven STIM1 intensity, with a punctate pattern (Figure 1F, bottom). The mean fluorescence intensity of STIM1 staining was increased in banded animals (Figure 1G). STIM1 protein, measured by Western analysis, was also increased in hypertrophied versus normal hearts (Online Figure I, B). Collectively, these studies show that STIM1 expression increases in feline ventricular myocytes with pressure overload-induced hypertrophy and suggest that STIM1 may oligomerize in these myocytes.

STIM1-Orai contributes to altered Ca²⁺ handling in hypertrophied myocytes

We have previously shown changes in contractile Ca²⁺ regulation in the hypertrophied feline ventricular myocytes^{38–40} which are consistent with the modifications in Ca²⁺ handling observed by other laboratories^{11, 41}. In the present study, we found that myocytes from banded animals had Ca²⁺ handling alterations consistent with previous reports, which includes reduced contraction magnitude, slowing of the systolic Ca²⁺ transient and shorter diastolic sarcomere lengths, under similar test conditions (Figure 2) and a prolonged AP duration (Figure 3). Hypertrophied feline ventricular myocytes exhibited spontaneous Ca²⁺ sparks during diastolic intervals between pacing-induced systolic Ca²⁺ transients (Figure 4). Ca²⁺ sparks were rarely present in normal feline myocytes under identical conditions (Figure 4). These results confirm and expand the data showing that the systolic and diastolic Ca²⁺ phenotype is disturbed in pathological pressure overload induced hypertrophied feline myocytes^{37, 38}.

The contribution of STIM1-Orai dependent Ca²⁺ influx to steady state myocyte contractions and Ca²⁺ transients was first explored by exposing isolated myocytes to the Orai blocker BTP2. This antagonist was chosen for its relative specificity for Orai over other ion channels⁴². Myocytes were incubated with either vehicle or BTP2, and then paced at 1Hz to measure steady state fractional shortening and Ca²⁺ transients. BTP2 did not significantly affect systolic Ca²⁺ transients or contractions in either normal (Online Figure II) or hypertrophied myocytes (Figure 2, A–I). However, BTP2 did cause an increase in diastolic sarcomere length in hypertrophied myocytes (Figure 2J).

The effects of BTP2 on action potential duration (APD) in sham and hypertrophied myocytes were determined using the voltage sensitive dye di-8-anneps. This method is technically less demanding than patch clamp approaches and allowed for study of an increased number of myocytes. In addition, this approach allowed for evaluation of AP waveform, without dialysis that could eliminate distinct intracellular contents in hypertrophied myocytes. Preliminary studies showed APs had similar waveforms and durations when recorded using either di-8-anneps or patch-clamp in myocytes (*not shown*). BTP2 had no effect on APD in sham myocytes, with a time to 90% repolarization (APD₉₀) of 285±9.5 ms (Figure 3). In contrast, myocytes from banded animals had longer baseline APDs and had significant APD shortening when incubated with BTP2, as compared to vehicle controls (APD₉₀: 434±11 ms vs 390±11.5 ms for vehicle and BTP2 respectively. *p* 0.01, Figure 3). In separate experiments, we found that BTP2 did not reduce Ca²⁺ current at the concentrations used in these experiments (Online Figure II, K).

Ca²⁺ sparks were quantified during the diastolic interval (1Hz) in sham and hypertrophied myocytes. Sparks were infrequently observed in sham myocytes but were routinely found in hypertrophied myocytes. BTP2 significantly reduced the number of sparks in hypertrophied myocytes as compared to vehicle control (Figure 4).

Increasing STIM1 Induces Ca²⁺ influx that loads the SR

To further explore the contribution of increased STIM1 expression to altered myocyte Ca²⁺ regulation in disease, adenoviral gene transfer was used to express STIM1 (human cDNA

clone) or red fluorescent protein (RFP) in freshly isolated adult feline myocytes (AFMs). Western blot and immunofluorescence confirmed increased expression of STIM1 within 12–18 hours of infection (Online Figure III). In these studies, STIM1 was found to be organized into puncta, similar to the staining pattern seen in hypertrophied myocytes.

AFMs and other myocytes from large mammals are electrically and mechanically quiescent in primary culture, and they maintain low cytoplasmic and SR Ca^{2+} ^{28, 43}. These properties result from the low cytoplasmic $[\text{Na}^+]$ in large mammalian ventricular myocytes, which produces forward mode $\text{Na}^+/\text{Ca}^{2+}$ exchanger (NCX) activity and low diastolic and SR $[\text{Ca}^{2+}]$ when not paced (Online Figure IV, A and B)³¹. These features are distinct from the conditions in rodent myocytes where high cytosolic $[\text{Na}^+]$ leads to persistent cytosolic and SR Ca^{2+} overload³¹. Unpaced AFMs with STIM1 expression exhibited higher SR loads than RFP myocytes (Online Figure IV, A and B). When paced, STIM1 myocytes had significantly increased Ca^{2+} transient amplitudes and decreased diastolic sarcomere lengths but increases in fractional myocyte failed to achieve statistical significance (Figure 5, A–E).

STIM1 could interact with a variety of sarcolemmal proteins to induce increased Ca^{2+} entry²³. Our results suggest that STIM1 interaction with Orai is the pathway for Ca^{2+} entry in unpaced myocytes that enhances diastolic SR Ca^{2+} loading. However, previous studies suggest that STIM1 can also directly interact with the L-type calcium channel (LTCC) and modify its behavior^{44, 45}, and this could alter myocyte Ca^{2+} . To test whether STIM1 interacted with LTCCs to alter SR loading, we exposed unpaced AFMs +/- STIM1 to verapamil, a potent LTCC blocker, and then induced SR Ca^{2+} release. Verapamil did not affect SR load in unpaced STIM1 expressing myocytes (Online Figure IV, A and B). Furthermore, we found that STIM1 expression did not alter LTCC current density, either at basal levels or after BAYK8644 treatment (Online Figure IV, C). However, STIM1 infected cells with increased Ca^{2+} transients had greater NCX activity (Online Figure IV, D).

It has been recently suggested that one function of STIM1 in cardiac myocytes is to interact with phospholamban (PLB) to enhance the activity of SERCA. We attempted to replicate this interaction by co-immunoprecipitating STIM1 with PLB. No interaction between STIM1 and PLB was found. We did observe SERCA2a immunoprecipitate with PLB, as expected⁴⁶ (Online Figure V). These results indicate that STIM1 does not interact with PLB in feline myocytes and suggest effects of STIM1 on Ca^{2+} influx are due to its interaction with sarcolemmal Orai channels.

Increased STIM1 expression is sufficient to induce diastolic sparks

STIM1 and RFP expressing myocytes were paced and diastolic Ca^{2+} sparks and sarcomere length were measured. A very low rate of spark activity was observed in RFP control myocytes (Figures 5F and 5G). STIM1 myocytes exhibited increased spark rates and a greater reduction in diastolic sarcomere length (Figure 5E). These changes mirrored the increased spark activity and reduced sarcomere length seen during diastole in myocytes from banded animals (Figure 4). BTP2 eliminated diastolic sparks in STIM1 myocytes (Figure 5F) but had no effects on RFP-infected myocytes (not shown), suggesting a role for STIM1-Orai dependent Ca^{2+} influx.

To independently test a role for Orai in diastolic Ca^{2+} sparks an Orai construct with a mutation in its pore forming region (E106Q), that blocks Ca^{2+} permeation was employed⁴⁷. This mutant will oligomerize with endogenous Orai channels (all isoforms), causing a dominant negative (dnOrai) effect, blocking all Orai channel activity⁴⁷. AFMs were infected with dn-Orai that was tagged with RFP, along with STIM1. These experiments showed that STIM1 was co-localized with dn-Orai in a punctated pattern along the sarcolemma (Figure 5H). Co-expression of dn-Orai with STIM1 prevented the increased diastolic spark rate caused by STIM1 alone (Figures 5F and 5G). Collectively, these results suggest that Orai is a necessary partner for STIM1 to cause Ca^{2+} influx in AFMs.

STIM1-Orai Mediated Ca^{2+} influx causes Ca^{2+} sparks and action potentials

AFMs expressing STIM1 exhibit spontaneous Ca^{2+} sparks and spontaneous contractions (Online Video I) while control myocytes were quiescent (Online Video II). To explore the bases of these spontaneous contractions we monitored membrane voltage using di-8-anneps. These experiments showed that STIM1 expressing myocytes demonstrate diastolic depolarization preceding spontaneous APs and contractions (Figure 6A), and these depolarizations are associated with spontaneous SR Ca^{2+} release. BTP2 treatment of STIM1 expressing myocytes blocked spontaneous APs and shortened the APD of paced myocytes (Figure 6B and 6C). These results are consistent with the idea that increased STIM1 expression produces Ca^{2+} influx through Orai, increasing SR Ca^{2+} loading that eventually results in spontaneous SR Ca^{2+} release (sparks). Spontaneous SR Ca^{2+} release is known to induce NCX-mediated inward current which can be sufficient to depolarize the membrane potential and trigger an AP⁴¹. These experiments also show that Ad-STIM1 infected AFMs could have sufficient numbers of Ca^{2+} sparks to elicit spontaneous APs (Figure 6A). Spontaneous Ca^{2+} sparks were not blocked by verapamil, confirming that STIM1 does not raise myocyte Ca^{2+} levels by altering the activity of LTCCs (Figures 6D and 6E). BTP2 and dn-Orai blocked resting sparks and spontaneous AP generation (Figures 6D and 6E).

STIM1 activation of Orai channels leads to CaMKII activation and cell death

Our experiments showed that STIM1 expression increased the rate of AFM death after 72 hours (20–40% viability) versus RFP-infected controls (80–90% viability, Figures 7A and 7B). We next explored the STIM1 membrane-signaling partner that is responsible for Ca^{2+} influx and cell death signaling in STIM1 infected AFMs. Our group and others have previously documented the importance of canonical transient receptor potential channels (TRPC) mediated Ca^{2+} influx in cell death signaling myocytes^{28, 48}. Some reports suggest that STIM1 can bind to and activate TRPC channels and induce Ca^{2+} influx⁴⁹. Previous work in our laboratory demonstrated that expression of a dominant negative TRPC4 construct (dn-TRPC4) results in total inhibition of all TRPC activity, through its oligomerization with each of the endogenous TRPC isoforms.²⁸ Using this same construct, we compared the effects of co-infection of STIM1 infected AFMs with either dn-TRPC4²⁸ or dnOrai. STIM1-induced cell death was not altered by dn-TRPC4 but was eliminated by dnOrai (Figure 7B). BTP2 also rescued the cell death phenotype of STIM1 myocytes (Figure 7B).

The link between increased Ca^{2+} influx and cell death signaling has also been shown to involve the activation of Ca^{2+} /calmodulin-dependent protein kinase II (CaMKII)⁵⁰. To test this idea STIM1 or RFP infected myocytes were treated with KN-93, a CaMKII inhibitor. KN-93 rescued myocytes from cell death, though not as completely as with BTP2 (Figure 7C). Collectively, these results indicate that increased STIM1-mediated Ca^{2+} entry can activate CaMKII, which likely contributes to both cell death and changes in myocyte Ca^{2+} handling. Additional evidence for this idea was that phospholamban (PLB) phosphorylation at threonine 17 (Thr-17, a CaMKII specific site) was found to be increased in STIM1 myocytes (Figure 7D). PLB-Thr-17 phosphorylation also can explain the accelerated tau of Ca^{2+} transient decay in STIM1-infected myocytes (Online Figure IV, E). BTP2 blocked STIM1 mediated PLB-T17 phosphorylation (Figure 7D), consistent with a central role of Orai. No changes in CaMKII autophosphorylation at Thr-286 or Thr-287 were observed by western blot (data not shown).

CaMKII activity has previously been shown to cause cell death by activating both apoptosis and necrosis in cardiac myocytes.⁵¹ To determine whether STIM1 causes apoptosis, caspase 3 cleavage was measured by Western analysis. No differences were found between STIM1 expressing myocytes and RFP controls (Online Figure VI) These results suggest that STIM1 activity can lead to necrotic cell death, similar to what we have seen when excess Ca^{2+} influx through the LTCC is induced³³.

DISCUSSION

SOCE and its effector proteins—STIM and Orai—are present in many tissue types where they regulate a number of different processes²³. In noncardiac cells, SOCE is activated after ER Ca^{2+} depletion and the resultant Ca^{2+} influx refills the ER stores²³. The presence and functional significance of SOCE in the normal adult heart is not well defined, but STIM expression in cardiac disease has been linked to pathological cardiac hypertrophy²⁷. The goal of the present study was to determine if Ca^{2+} influx through a STIM and Orai-dependent pathway contributes to the electromechanical phenotype of either normal or hypertrophied ventricular myocytes. A novel aspect of our study was that two independent approaches, pharmacologic (BTP2) Orai blockade and genetic (dnOrai) manipulation were used to demonstrate phenotypic features that were dependent on Orai channel function. Our experiments showed that both STIM1/2 and Orai1/3 are expressed in normal feline myocytes but are not major contributors to the phenotypic features we measured in this study (Online Figure II). Therefore, their function in the normal heart is yet to be defined. STIM/Orai contributions to electromechanical remodeling in hypertrophied hearts were studied in ventricular myocytes isolated from feline hearts with slow, progressive pressure overload (aortic banding). Myocytes isolated from hypertrophied hearts exhibited increased STIM1 expression, similar to previous reports²⁹. Our novel findings include the observation that STIM1 was organized into puncta, indicating STIM1 activation in hypertrophied myocytes (Figure 1F). Blockade of ion flux through STIM1/Orai with BTP2 in hypertrophied myocytes revealed, for the first time, that STIM1/Orai activity contributes to APD prolongation (Figure 3). In addition, we made the novel observation that STIM1-Orai activity leads to diastolic Ca^{2+} sparks and a shortening of the diastolic sarcomere length (Figures 2 and 4). Additional experiments with cultured adult feline myocytes (AFMs)

showed that increasing STIM1 expression was sufficient to induce persistent Ca^{2+} influx and recapitulated many of the phenotypic features of hypertrophied myocytes. Specifically, STIM1 expression induced Ca^{2+} influx caused spontaneous Ca^{2+} sparks, shortening of diastolic sarcomere length, SR Ca^{2+} loading, and spontaneous APs (Figure 5). STIM1 expression was also linked to cell death, in part by activating CaMKII (Figure 7C). Our studies with BTP2 and dnOrai, two reagents that have not previously been used to investigate Ca^{2+} handling in ventricular cardiac myocytes, demonstrate that Ca^{2+} entry into hypertrophied ventricular myocytes through a STIM1-Orai pathway contribute to those phenotypic features of diseased myocytes that have been linked to lethal arrhythmias, contractile dysfunction and myocyte death signaling.

Expression and activity of STIM and Orai in normal cardiac myocytes

The nature of SOCE in normal adult cardiac myocytes from a variety of species has been investigated by many laboratories and found to be very small or undetectable^{16, 19, 27}. However, myocyte STIM1 knockout leads to aberrant cardiac structure and function⁵². Therefore, STIM1 clearly has roles that are yet to be defined. The experiments performed in the current study support the idea that STIM-Orai activity makes little or no contribution to the electromechanical function of normal ventricular myocytes. BTP2, a potent SOCE (Orai) blocker^{23, 53}, did not modify APD, Ca^{2+} transients or contractions of normal myocytes (Figures 2 and 3 and Online Figure II). These data suggest that STIM and Orai proteins, while present in the normal heart, have little or no effects on Ca^{2+} cycling. The reason(s) for the absence of detectable activation of STIM1-Orai in normal myocytes is unclear and requires additional study. For example, there is some evidence that STIM1 can be activated by ROS or pH changes, independent of the level of SR [Ca^{2+}] stores²⁵ and these issues were not examined. It is also possible that STIM and Orai have functional roles in the normal heart beyond the electromechanical features that we primarily examined.

STIM-Orai form a Ca^{2+} Influx pathway that contributes to electromechanical remodeling in hypertrophy

STIM1 expression increases after pressure overload^{19, 27, 29} and the resultant Ca^{2+} influx is thought to be involved in the induction of pathological hypertrophy. STIM1 may be part of the fetal gene program that becomes reactivated during pathological stress and could contribute a pool of Ca^{2+} that activates pathological hypertrophy signaling. Reduction of STIM1 levels has been shown to reduce hypertrophic signaling in both neonatal and adult rodent myocytes^{19, 27, 54}. Increased expression of STIM1 conversely resulted in an exaggerated hypertrophic response to TAC, MI, and chronic isoproterenol infusion in rodents²⁹. Collectively, these studies support the idea that STIM1 expression and activity increase in myocytes responding to persistent pathological stress, and the resultant response includes myocyte hypertrophy.

The direct contribution of STIM1-Orai dependent Ca^{2+} influx to the distinctive electromechanical phenotype of the hypertrophied ventricular myocytes has not been well studied and was the topic of this study. A feline model of slow progressive pressure overload that has critical features of human diseases, including concentric LV hypertrophy without systolic dysfunction (Figure 1) was employed. This model has many features of a human

condition called heart failure with preserved ejection fraction (HFpEF)^{55, 56}, with increases in ventricular wall thickness and HW/BW (Figure 1C and 1D) without cardiac dilation or reductions in systolic function (Figure 1B). In myocytes from banded animals, STIM1 mRNA and protein was increased along with a small but significant increase in Orai3 mRNA (Figure 1E). It is possible that the Orai3 isoform is the major partner for STIM1 in cardiac disease, as found by others¹⁷. Future studies should focus on how the unique properties of Orai3 contribute to the electromechanical features of hypertrophied myocytes.

In myocytes from normal animals, immunofluorescence staining revealed that STIM1 is localized uniformly in the SR membrane along the Z-line (Online Figure I) but in banded myocytes exhibited a punctated pattern (Figure 1F), indicative of STIM1 oligomerization²⁵. These results support the idea that STIM1 is increased in abundance and activated in the hypertrophied heart.

A contractile role for STIM and Orai in hypertrophy

Alterations in myocyte Ca²⁺ handling are central to the development of the electromechanical phenotype of the diseased heart¹¹. The idea that Ca²⁺ entry through a STIM1-Orai complex contributes to phenotypic adaptation in disease has not, to our knowledge been studied in detail previously, especially in animal models with electromechanical properties similar to those in the human heart. To investigate whether increased STIM1-Orai activity contributes to contractile abnormalities in feline hypertrophy, we first employed BTP2 to block Orai channels. In comparison to other SOCE antagonists, BTP2 has little affinity for LTCCs⁵⁷ (Online Figure II, K) and potassium channels⁴². BTP2 had no effects on APs, Ca²⁺ transients or contractions in normal myocytes, consistent with little or no STIM1-Orai activity in the normal heart and also documenting the lack of off target effects under the conditions we employed (Online Figure II).

The phenotypic features of hypertrophied AFMs included prolongation of the APD, slowing and prolongation of the Ca²⁺ transient, reductions of diastolic sarcomere length, increases in diastolic spark rate and prolongation of contraction (Figures 2, 3 and 4). These changes result from modifications in the abundance and behavior of many molecules that participate in contraction²⁶. To define a contribution of STIM1-Orai in these complex adaptations, hypertrophied AFMs were treated with BTP2. These studies showed that BTP2 shortened the APD, reduced diastolic spark rates and produced a lengthening of diastolic sarcomere length, but had no significant effects on steady state Ca²⁺ transients (Figures 2, 3 and 4). A major advantage of using the feline model to explore STIM-Orai contributions to APD is the low membrane conductance during their human-like AP plateau phase¹³. The high conductance state during repolarization of rodent APs masks changes in small currents that could make important contributions to changes in APD in human disease^{12, 13}.

Our results suggest that BTP2 blocks a small amount of Ca²⁺ entry through a STIM-Orai channel complex in hypertrophied AFMs that contributes to APD prolongation in hypertrophied AFMs. Our results also suggest that this Ca²⁺ influx can contribute to diastolic SR Ca²⁺ leak (Ca²⁺ sparks) that can reduce diastolic sarcomere length. Collectively, these data are consistent with the idea that increased STIM1/Orai activity in hypertrophy contributes to the electromechanical phenotype of hypertrophied AFMs.

STIM1/Orai regulate SR Ca²⁺

Studies in genetically modified mice strongly support the idea that STIM1 expression is linked to cardiac hypertrophy¹⁹, likely through activation of SOCE. However, these studies do not directly link STIM1 to functional changes, since these could be secondary to the hypertrophy rather than directly resulting from STIM1 activity. To directly link the contributions of increased STIM1 expression/activity to myocyte electromechanical properties, we acutely expressed STIM1 in cultured AFMs. This model system allowed us to manipulate levels of STIM1 with minimal compensatory changes in global gene expression, which often occurs in genetic mouse models or in any model of induced disease. STIM1 was organized into puncta (Online Figure III, B) in STIM1 expressing AFMs, comparable to the pattern observed in myocytes from banded animals. Acute STIM1 expression caused several functional alterations that paralleled changes observed in hypertrophied feline myocytes, including Ca²⁺ sparks during the diastolic period in paced myocytes (Figure 5F), prolonged APs (Figure 6B), and increased NCX-mediated Ca²⁺ efflux (Online Figure IV, D). These alterations were reduced, both in-vitro and in freshly isolated hypertrophied myocytes, when cells were treated with BTP2, supporting a direct role of STIM1-Orai.

Cultured AFMs normally maintain low cytosolic and SR [Ca²⁺]²⁸. Expressing STIM1 caused an increase in SR Ca²⁺ stores (Online Figure IV) and this is the likely basis for their increased Ca²⁺ spark rate and spontaneous, SR Ca²⁺ release dependent spontaneous APs. STIM1 might also induce abnormal SR Ca²⁺ release by influencing the [Ca²⁺] within the diffusion limiting cleft between the T-tubule and SR membranes⁴¹ or by altering the properties of ryanodine receptors, possibly by CaMKII-mediated phosphorylation, which we showed was increased in STIM1 myocytes. A recent study in cultured rodent ventricular myocytes suggests that expressed STIM1 interacts with phospholamban (PLB) to alter SR Ca²⁺ uptake and induce SR Ca²⁺ sparks¹⁶. We explored this possibility by examining the interaction between PLB and STIM1 using coimmunoprecipitation approaches (Online Figure V), but could find no evidence to support this hypothesis.

STIM1 expression can cause AFM necrosis

Our in-vitro studies show that STIM1 expression increased the rate of AFM death (Figure 7). STIM1 infected AFMs did not appear to die via apoptosis, suggestive of a necrotic process. We have previously found that persistent increases in Ca²⁺ influx via the LTCC induces a necrotic cell death in genetically modified mice^{58, 59}. The cell death effects of STIM1 were abolished by BTP2 and dnOrai, documenting a role for Ca²⁺ influx via the STIM-Orai complex. Activation of CaMKII was also shown to be involved in this cell death effect (Figure 7D and 7E). These results warrant further exploration, as increased cell death in vivo would contribute to cardiac fibrosis and compensatory hypertrophy by the remaining myocytes, which may be partly responsible for the hypertrophy induced by STIM1 that others have observed¹⁹.

In summary, the present study shows that pathological hypertrophy is associated with increases in STIM1 expression in AFMs. Our results are consistent with the idea that STIM1 associates with sarcolemmal Orai channels to produce Ca²⁺ influx that prolongs the APD, helps maintain SR Ca²⁺ load, but induces SR Ca²⁺ leak (Ca²⁺ sparks) and reduced diastolic

sarcomere length. These changes likely contribute to disturbed Ca^{2+} regulation, Ca^{2+} dependent arrhythmias and cell death in the diseased heart. Our findings suggest that STIM1-Orai activity increases in myocytes from hearts with disease-related increases in the contractile demands of the heart. Collectively, our findings suggest STIM-Orai mediated Ca^{2+} influx directly contributes to both the induction of pathological hypertrophy as well as the aberrant electromechanical phenotype of the hypertrophied heart, making this complex an attractive therapeutic target.

Supplementary Material

Refer to Web version on PubMed Central for supplementary material.

Acknowledgments

SOURCES OF FUNDING

Supported by NIH grants to SRH. SM supported by SDG from AHA.

Nonstandard Abbreviations and Acronyms

AP	Action Potential
APD	Action Potential Duration
APD90	Time to 90% Action Potential repolarization
CaMKII	Calcium/Calmodulin-Dependent Protein Kinase II
dnOrai	Dominant Negative Orai
ER	Endoplasmic Reticulum
HW/BW	Heart Weight to Body Weight Ratio
LVH	Left Ventricular Hypertrophy
LTCC	L-type Calcium Channel
NCX	Sodium/Calcium Exchanger
PLB	Phospholamban
RFP	Red Fluorescent Protein
ROS	Reactive Oxygen Species
RT-PCR	Real Time Polymerase Chain Reaction
SOCE	Store Operated Calcium Entry
SR	Sarcoplasmic Reticulum
STIM	Stromal Interaction Molecule 1

TRPC Transient Receptor Potential, Canonical type

Thr-17 Threonine 17

References

1. Dodge HT. Functional characteristics of the left ventricle in heart disease. *Annals of internal medicine*. 1968; 69:941–8. [PubMed: 4235255]
2. Kennedy JW, Twiss RD, Blackmon JR, Dodge HT. Quantitative angiocardiology. 3. Relationships of left ventricular pressure, volume, and mass in aortic valve disease. *Circulation*. 1968; 38:838–45. [PubMed: 4235191]
3. Zaino EC, Tabor SH. Cardiac Hypertrophy in Acute Myocardial Infarction. A study Based on 100 Autopsied Cases. *Circulation*. 1963; 28:1081–3. [PubMed: 14082921]
4. Sampson KJ, Kass RS. Molecular mechanisms of adrenergic stimulation in the heart. *Heart Rhythm*. 2010; 7:1151–1153. [PubMed: 20156590]
5. Grossman W, Jones D, McLaurin LP. Wall stress and patterns of hypertrophy in the human left ventricle. *Journal of Clinical Investigation*. 1975; 56:56–64. [PubMed: 124746]
6. MacLellan WR, Schneider MD. Genetic dissection of cardiac growth control pathways. *Annual review of physiology*. 2000; 62:289–319.
7. Goonasekera SA, Molkentin JD. Unraveling the secrets of a double life: contractile versus signaling Ca²⁺ in a cardiac myocyte. *Journal of molecular and cellular cardiology*. 2012; 52:317–22. [PubMed: 21600216]
8. Makarewich CA, Correll RN, Gao H, Zhang H, Yang B, Berretta RM, Rizzo V, Molkentin JD, Houser SR. A caveolae-targeted L-type Ca²⁺ channel antagonist inhibits hypertrophic signaling without reducing cardiac contractility. *Circ Res*. 2012; 110:669–74. [PubMed: 22302787]
9. Wu X, Eder P, Chang B, Molkentin JD. TRPC channels are necessary mediators of pathologic cardiac hypertrophy. *Proc Natl Acad Sci U S A*. 107:7000–5.
10. Luo M, Anderson ME. Mechanisms of altered Ca²⁺(+) handling in heart failure. *Circ Res*. 2013; 113:690–708. [PubMed: 23989713]
11. Houser SR, Piacentino V 3rd, Weissner J. Abnormalities of calcium cycling in the hypertrophied and failing heart. *Journal of molecular and cellular cardiology*. 2000; 32:1595–607. [PubMed: 10966823]
12. Pogwizd SM, Schlotthauer K, Li L, Yuan W, Bers DM. Arrhythmogenesis and contractile dysfunction in heart failure: Roles of sodium-calcium exchange, inward rectifier potassium current, and residual beta-adrenergic responsiveness. *Circ Res*. 2001; 88:1159–67. [PubMed: 11397782]
13. Nattel S, Maguy A, Le Bouter S, Yeh YH. Arrhythmogenic ion-channel remodeling in the heart: heart failure, myocardial infarction, and atrial fibrillation. *Physiological reviews*. 2007; 87:425–56. [PubMed: 17429037]
14. Levy D, Garrison RJ, Savage DD, Kannel WB, Castelli WP. Prognostic implications of echocardiographically determined left ventricular mass in the Framingham Heart Study. *The New England journal of medicine*. 1990; 322:1561–6. [PubMed: 2139921]
15. Haider AW, Larson MG, Benjamin EJ, Levy D. Increased left ventricular mass and hypertrophy are associated with increased risk for sudden death. *Journal of the American College of Cardiology*. 1998; 32:1454–1459. [PubMed: 9809962]
16. Zhao G, Li T, Brochet DX, Rosenberg PB, Lederer WJ. STIM1 enhances SR Ca²⁺ content through binding phospholamban in rat ventricular myocytes. *Proc Natl Acad Sci U S A*. 2015; 112:E4792–801. [PubMed: 26261328]
17. Saliba Y, Keck M, Marchand A, Atassi F, Ouille A, Cazorla O, Trebak M, Pavoine C, Lacampagne A, Hulot JS, Fares N, Fauconnier J, Lompre AM. Emergence of Orai3 activity during cardiac hypertrophy. *Cardiovascular research*. 2015; 105:248–59. [PubMed: 25213556]
18. Luo X, Hojavey B, Jiang N, Wang ZV, Tandan S, Rakalin A, Rothermel BA, Gillette TG, Hill JA. STIM1-dependent store-operated Ca²⁺(+) entry is required for pathological cardiac hypertrophy. *Journal of molecular and cellular cardiology*. 2012; 52:136–47. [PubMed: 22108056]

19. Hulot JS, Fauconnier J, Ramanujam D, Chaanine A, Aubart F, Sassi Y, Merkle S, Cazorla O, Ouille A, Dupuis M, Hadri L, Jeong D, Muhlstedt S, Schmitt J, Braun A, Benard L, Saliba Y, Laggerbauer B, Nieswandt B, Lacampagne A, Hajjar RJ, Lompre AM, Engelhardt S. Critical role for stromal interaction molecule 1 in cardiac hypertrophy. *Circulation*. 2011; 124:796–805. [PubMed: 21810664]
20. Liou J, Kim ML, Heo WD, Jones JT, Myers JW, Ferrell JE Jr, Meyer T. STIM is a Ca²⁺ sensor essential for Ca²⁺-store-depletion-triggered Ca²⁺ influx. *Current biology : CB*. 2005; 15:1235–41. [PubMed: 16005298]
21. Roos J, DiGregorio PJ, Yeromin AV, Ohlsen K, Lioudyno M, Zhang S, Safrina O, Kozak JA, Wagner SL, Cahalan MD, Velicelebi G, Stauderman KA. STIM1, an essential and conserved component of store-operated Ca²⁺ channel function. *The Journal of cell biology*. 2005; 169:435–45. [PubMed: 15866891]
22. Soboloff J, Spassova MA, Hewavitharana T, He LP, Xu W, Johnstone LS, Dziadek MA, Gill DL. STIM2 is an inhibitor of STIM1-mediated store-operated Ca²⁺ Entry. *Current biology : CB*. 2006; 16:1465–70. [PubMed: 16860747]
23. Prakriya M, Lewis RS. Store-Operated Calcium Channels. *Physiological reviews*. 2015; 95:1383–436. [PubMed: 26400989]
24. Salido GM, Sage SO, Rosado JA. Biochemical and functional properties of the store-operated Ca²⁺ channels. *Cellular signalling*. 2009; 21:457–61. [PubMed: 19049864]
25. Soboloff J, Rothberg BS, Madesh M, Gill DL. STIM proteins: dynamic calcium signal transducers. *Nat Rev Mol Cell Biol*. 2012; 13:549–65. [PubMed: 22914293]
26. Bers DM. Cardiac excitation-contraction coupling. *Nature*. 2002; 415:198–205. [PubMed: 11805843]
27. Luo X, Hojayeve B, Jiang N, Wang ZV, Tandan S, Rakalin A, Rothermel BA, Gillette TG, Hill JA. STIM1-dependent Store-Operated Ca(2+) Entry is Required for Pathological Cardiac Hypertrophy. *Journal of molecular and cellular cardiology*. 2012; 52:136–147. [PubMed: 22108056]
28. Makarewich CA, Zhang H, Davis J, Correll RN, Trapanese DM, Hoffman NE, Troupes CD, Berretta RM, Kubo H, Madesh M, Chen X, Gao E, Molkentin JD, Houser SR. Transient receptor potential channels contribute to pathological structural and functional remodeling after myocardial infarction. *Circulation research*. 2014; 115:567–80. [PubMed: 25047165]
29. Correll RN, Goonasekera SA, van Berlo JH, Burr AR, Accornero F, Zhang H, Makarewich CA, York AJ, Sargent MA, Chen X, Houser SR, Molkentin JD. STIM1 elevation in the heart results in aberrant Ca(2)(+) handling and cardiomyopathy. *Journal of molecular and cellular cardiology*. 2015; 87:38–47. [PubMed: 26241845]
30. Bers, DM. *Excitation-Contraction Coupling and Cardiac Contractile Force*. 2nd. Dordrecht, The Netherlands: Kluwer Academic Publishers; 2001.
31. Bers DM. Cardiac Na/Ca exchange function in rabbit, mouse and man: what's the difference? *Journal of molecular and cellular cardiology*. 2002; 34:369–73. [PubMed: 11991726]
32. Harris DM, Mills GD, Chen X, Kubo H, Berretta RM, Votaw VS, Santana LF, Houser SR. Alterations in early action potential repolarization causes localized failure of sarcoplasmic reticulum Ca²⁺ release. *Circ Res*. 2005; 96:543–50. [PubMed: 15705962]
33. Chen X, Zhang X, Kubo H, Harris DM, Mills GD, Moyer J, Berretta R, Potts ST, Marsh JD, Houser SR. Ca²⁺ Influx-Induced Sarcoplasmic Reticulum Ca²⁺ Overload Causes Mitochondrial-Dependent Apoptosis in Ventricular Myocytes. *Circulation Research*. 2005; 97:1009–1017. [PubMed: 16210547]
34. Pollack PS, Carson NL, Nuss HB, Marino TA, Houser SR. Mechanical properties of adult feline ventricular myocytes in culture. *American Journal of Physiology – Heart and Circulatory Physiology*. 1991; 260:H234–H241.
35. Mitcheson JS, Hancox JC, Levi AJ. Action potentials, ion channel currents and transverse tubule density in adult rabbit ventricular myocytes maintained for 6 days in cell culture. *Pflügers Archiv*. 1996; 431:814–827. [PubMed: 8927497]
36. Mills GD, Kubo H, Harris DM, Berretta RM, Piacentino V 3rd, Houser SR. Phosphorylation of phospholamban at threonine-17 reduces cardiac adrenergic contractile responsiveness in chronic

- pressure overload-induced hypertrophy. *Am J Physiol Heart Circ Physiol.* 2006; 291:H61–70. [PubMed: 16772527]
37. Bailey BA, Houser SR. Calcium transients in feline left ventricular myocytes with hypertrophy induced by slow progressive pressure overload. *Journal of molecular and cellular cardiology.* 1992; 24:365–73. [PubMed: 1535666]
 38. Bailey BA, Houser SR. Sarcoplasmic reticulum-related changes in cytosolic calcium in pressure-overload-induced feline LV hypertrophy. *Am J Physiol.* 1993; 265:H2009–16. [PubMed: 8285239]
 39. Nuss HB, Houser SR. T-type Ca²⁺ current is expressed in hypertrophied adult feline left ventricular myocytes. *Circ Res.* 1993; 73:777–82. [PubMed: 8396509]
 40. Kleiman RB, Houser SR. Calcium currents in normal and hypertrophied isolated feline ventricular myocytes. *Am J Physiol.* 1988; 255:H1434–42. [PubMed: 2849320]
 41. Bers DM. Cardiac sarcoplasmic reticulum calcium leak: basis and roles in cardiac dysfunction. *Annual review of physiology.* 2014; 76:107–27.
 42. Zitt C, Strauss B, Schwarz EC, Spaeth N, Rast G, Hatzelmann A, Hoth M. Potent inhibition of Ca²⁺ release-activated Ca²⁺ channels and T-lymphocyte activation by the pyrazole derivative BTP2. *J Biol Chem.* 2004; 279:12427–37. [PubMed: 14718545]
 43. Pollack PS, Carson NL, Nuss HB, Marino TA, Houser SR. Mechanical properties of adult feline ventricular myocytes in culture. *Am J Physiol.* 1991; 260:H234–41. [PubMed: 1992803]
 44. Park CY, Shcheglovitov A, Dolmetsch R. The CRAC Channel Activator STIM1 Binds and Inhibits L-Type Voltage-Gated Calcium Channels. *Science.* 2010; 330:101–105. [PubMed: 20929812]
 45. Wang Y, Deng X, Mancarella S, Hendron E, Eguchi S, Soboloff J, Tang XD, Gill DL. The calcium store sensor, STIM1, reciprocally controls Orai and CaV1.2 channels. *Science.* 2010; 330:105–9. [PubMed: 20929813]
 46. Asahi M, McKenna E, Kurzydowski K, Tada M, MacLennan DH. Physical interactions between phospholamban and sarco(endo)plasmic reticulum Ca²⁺-ATPases are dissociated by elevated Ca²⁺, but not by phospholamban phosphorylation, vanadate, or thapsigargin, and are enhanced by ATP. *J Biol Chem.* 2000; 275:15034–8. [PubMed: 10809745]
 47. Prakriya M, Feske S, Gwack Y, Srikanth S, Rao A, Hogan PG. Orai1 is an essential pore subunit of the CRAC channel. *Nature.* 2006; 443:230–3. [PubMed: 16921383]
 48. Shan D, Marchase RB, Chatham JC. Overexpression of TRPC3 increases apoptosis but not necrosis in response to ischemia-reperfusion in adult mouse cardiac myocytes. *American Journal of Physiology – Cell Physiology.* 2008; 294:C833–C841. [PubMed: 18184877]
 49. Yuan JP, Zeng W, Huang GN, Worley PF, Muallem S. STIM1 heteromultimerizes TRPC channels to determine their function as store-operated channels. *Nature cell biology.* 2007; 9:636–45. [PubMed: 17486119]
 50. Erickson JR, He BJ, Grumbach IM, Anderson ME. CaMKII in the Cardiovascular System: Sensing Redox States. *Physiological reviews.* 2011; 91:889–915. [PubMed: 21742790]
 51. Vila-Petroff M, Salas MA, Said M, Valverde CA, Sapia L, Portiansky E, Hajjar RJ, Kranias EG, Mundiña-Weilenmann C, Mattiazzi A. CaMKII inhibition protects against necrosis and apoptosis in irreversible ischemia-reperfusion injury. *Cardiovascular research.* 2007; 73:689–698. [PubMed: 17217936]
 52. Collins HE, He L, Zou L, Qu J, Zhou L, Litovsky SH, Yang Q, Young ME, Marchase RB, Chatham JC. Stromal interaction molecule 1 is essential for normal cardiac homeostasis through modulation of ER and mitochondrial function. *Am J Physiol Heart Circ Physiol.* 2014; 306:H1231–9. [PubMed: 24585777]
 53. Ohga K, Takezawa R, Arakida Y, Shimizu Y, Ishikawa J. Characterization of YM-58483/BTP2, a novel store-operated Ca²⁺ entry blocker, on T cell-mediated immune responses in vivo. *International immunopharmacology.* 2008; 8:1787–92. [PubMed: 18793756]
 54. Voelkers M, Salz M, Herzog N, Frank D, Dolatabadi N, Frey N, Gude N, Friedrich O, Koch WJ, Katus HA, Sussman MA, Most P. Orai1 and Stim1 regulate normal and hypertrophic growth in cardiac myocytes. *Journal of molecular and cellular cardiology.* 2010; 48:1329–34. [PubMed: 20138887]
 55. Borlaug BA, Paulus WJ. Heart failure with preserved ejection fraction: pathophysiology, diagnosis, and treatment. *European Heart Journal.* 2011; 32:670–679. [PubMed: 21138935]

56. Braunwald E. Heart Failure. *JACC: Heart Failure*. 2013; 1:1–20. [PubMed: 24621794]
57. Ishikawa J, Ohga K, Yoshino T, Takezawa R, Ichikawa A, Kubota H, Yamada T. A pyrazole derivative, YM-58483, potently inhibits store-operated sustained Ca²⁺ influx and IL-2 production in T lymphocytes. *J Immunol*. 2003; 170:4441–9. [PubMed: 12707319]
58. Chen X, Nakayama H, Zhang X, Ai X, Harris DM, Tang M, Zhang H, Szeto C, Stockbower K, Berretta RM, Eckhart AD, Koch WJ, Molkentin JD, Houser SR. Calcium influx through Cav1.2 is a proximal signal for pathological cardiac myocyte hypertrophy. *Journal of molecular and cellular cardiology*. 2011; 50:460–70. [PubMed: 21111744]
59. Nakayama H, Chen X, Baines CP, Klevitsky R, Zhang X, Zhang H, Jaleel N, Chua BH, Hewett TE, Robbins J, Houser SR, Molkentin JD. Ca²⁺- and mitochondrial-dependent cardiac myocyte necrosis as a primary mediator of heart failure. *J Clin Invest*. 2007; 117:2431–44. [PubMed: 17694179]

NOVELTY AND SIGNIFICANCE

What Is Known?

- Stromal interaction molecule 1 (STIM1) in the endo (sarco) plasmic reticulum (SR) partners with surface membrane Orai calcium (Ca^{2+}) channels to regulate SR Ca^{2+} stores in a variety of cell types.
- Pathological cardiac hypertrophy with mechanical dysfunction are associated with disturbed Ca^{2+} regulation.
- Increased STIM1 expression contributes to cardiac hypertrophy.

What New Information Does This Article Contribute?

- STIM1 partners with Orai channels in hypertrophied cardiac myocytes to produce Ca^{2+} influx and increase SR Ca^{2+} stores.
- STIM1-mediated Ca^{2+} influx contributes to action potential prolongation, dyssynchronous Ca^{2+} release (sparks), and cell death in hypertrophied cardiac myocytes.

Ca^{2+} levels in cardiac myocytes regulate contractile function and influence a host of normal and pathological processes. In cardiac hypertrophy Ca^{2+} regulation is deranged and produces altered electrical and mechanical function. Increased expression of STIM1 in the heart has been linked to the development of pathological hypertrophy, but the contribution of this putative Ca^{2+} influx pathway to hypertrophic electromechanical disturbances is unknown. Here, we used genetic and pharmacologic approaches to define the role of STIM1 to the electromechanical alterations of hypertrophied myocytes. The results of these experiments showed that STIM1 partners with Orai channels to produce a Ca^{2+} influx pathway. STIM1-mediated Ca^{2+} influx contributed to prolonged action potential duration, caused SR Ca^{2+} overload and associated Ca^{2+} sparks during diastole to shorten diastolic sarcomere length, and could induce necrotic myocyte death. STIM1-Orai was not shown to make significant contributions to the electromechanical properties of normal myocytes. These findings show that STIM1-Orai-mediated Ca^{2+} influx in hypertrophied cardiac myocytes contributes to the electromechanical derangements that can cause lethal cardiac arrhythmias and depressed cardiac pump function.

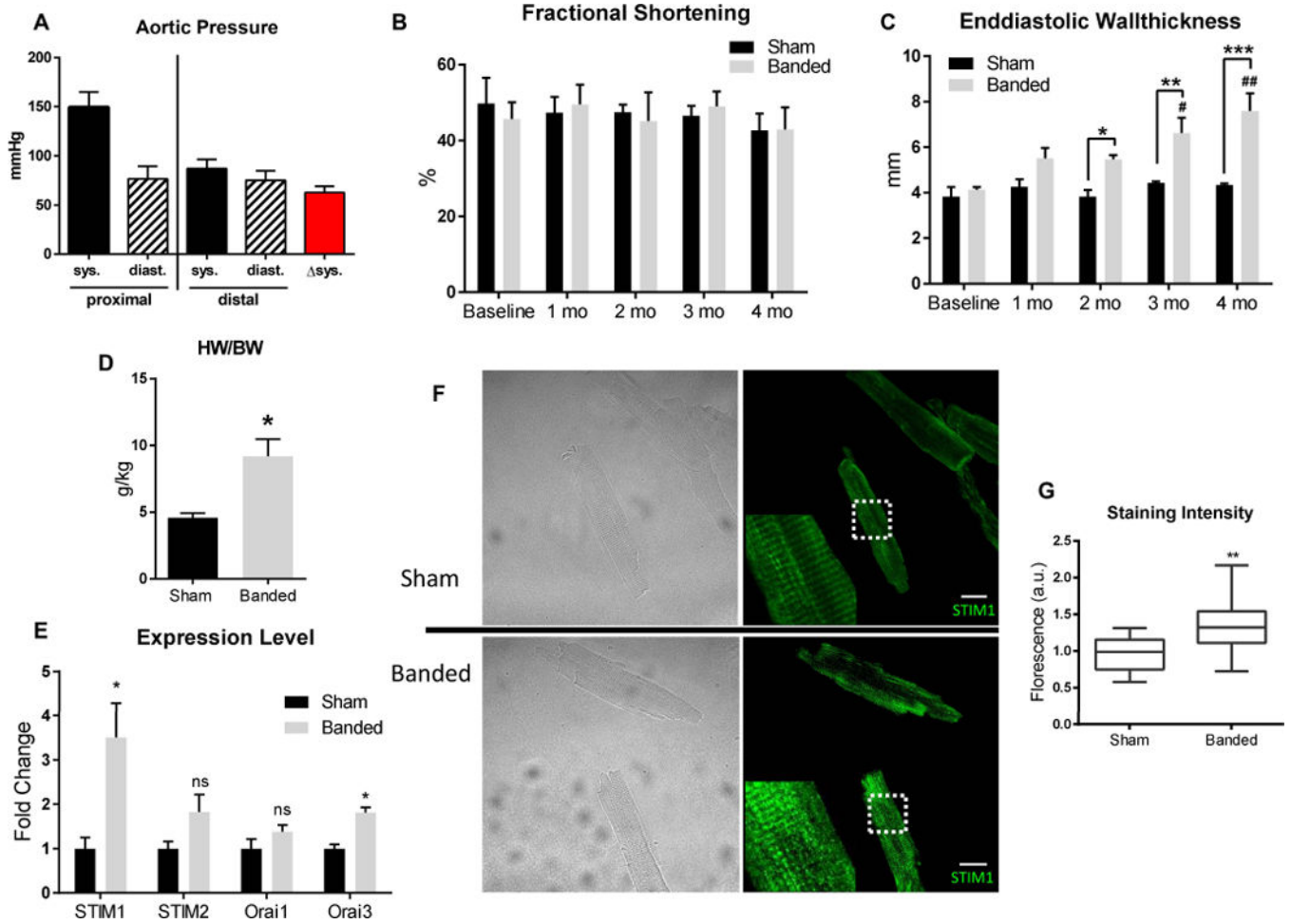


Figure 1. Expression of STIM and Orai in Hypertrophy

A, Proximal and distal pressures and the difference (Δ sys) across the aortic band after 4 months, measured using a pressure catheter (n=4) **B**, Fractional shortening measured by echocardiography over 4 months (n=4 each group). **C**, End-diastolic wall thickness measured by echocardiography over 4 months (n=4 each group). **D**, Heart weight to body weight ratio (HW/BW) in sham and banded animals (n=4 each group). **E**, mRNA levels were measured by RT-PCR in myocytes isolated from sham and banded animals after 4 months, normalized by GAPDH expression (n=4 each group). **F**, Transmitted light and STIM1 immunofluorescence staining in isolated myocytes from sham and banded animals. *Scale bar = 25 μ m*. **G**, Average fluorescence intensity of myocytes stained for STIM1 (n=4 animals each group, 38–42 myocytes). (**p* 0.05 vs Sham, ***p* 0.01 vs sham, (***)*p* 0.001 vs Sham #*p* 0.001 vs Baseline, ##*p* 0.0001 vs Baseline)

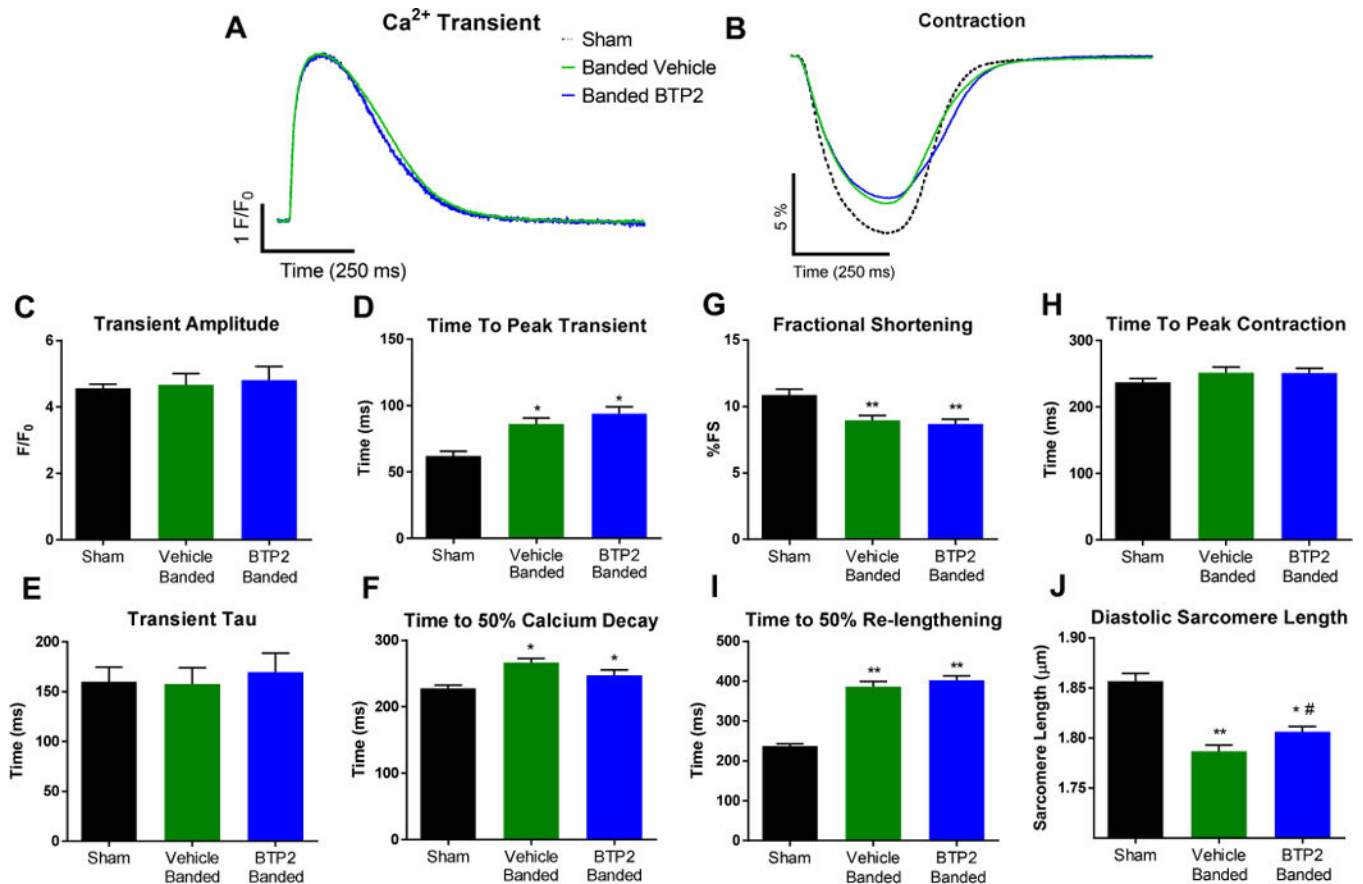


Figure 2. Ca²⁺ Transients and Contractions in Sham and Banded Animals Treated with BTP2
A, Ca²⁺ transients, displayed as F/F₀ of myocytes paced at 1Hz with field stimulation. **B**, Sarcomere length traces of myocytes paced at 1Hz. **C**, Peak transient amplitude. **D**, Time to peak transient amplitude after stimulation. **E**, Tau time constant of the transient decline. **F**, Time from initial stimulation to 50% Ca²⁺ decay from peak amplitude. **G**, Maximal shortening from baseline length. **H**, Time to peak contraction. **I**, Time to 50% re-lengthening from peak contraction. **J**, Average sarcomere length during diastole. (n=4 animals each group, 20–30 myocytes). (**p* 0.05 vs. control, ***p* 0.01 vs control, # *p* 0.05 vs vehicle-banded).

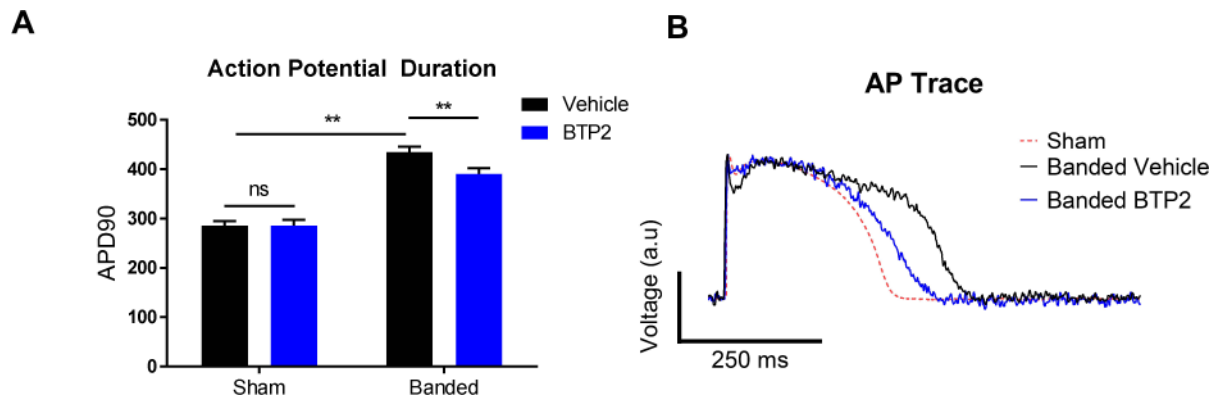


Figure 3. Action Potentials Recorded from Sham and Banded Myocytes Treated with BTP2
A, Time to 90% repolarization of APs in myocytes from sham or banded animals, with or without BTP2. **B**, Trace recording of di-8-anneps fluorescence indicating voltage change during field stimulation at 1Hz (n=4 animals each group, 30–40 myocytes). (***p* 0.01)

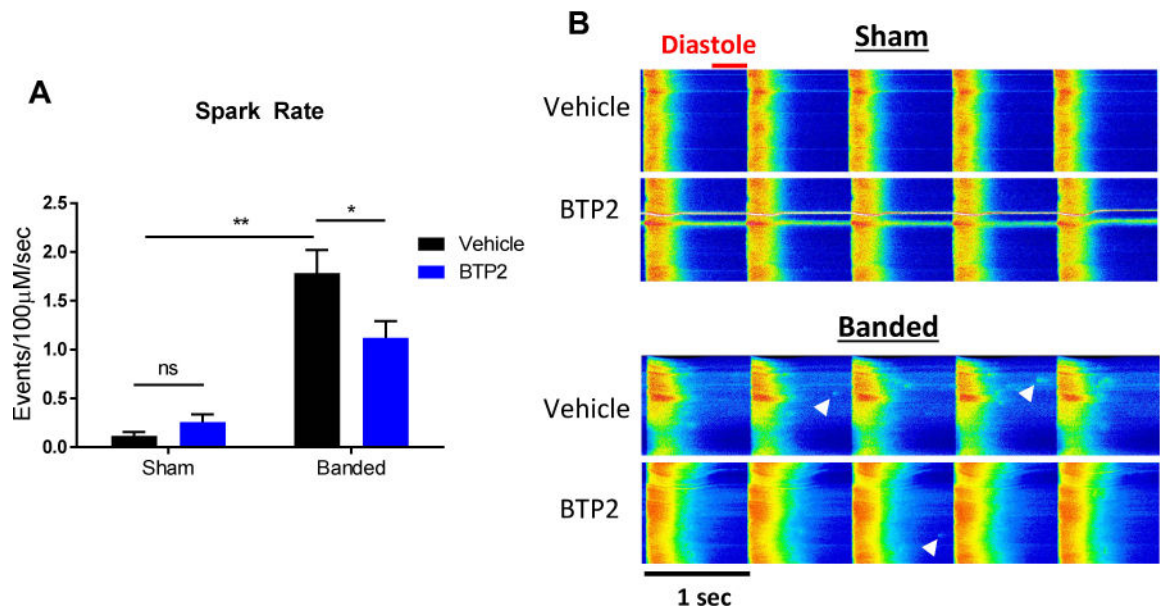


Figure 4. Diastolic Ca^{2+} Sparks Are Inhibited by BTP2 in Hypertrophic Myocytes
A, Spark rates during diastole in sham and banded myocytes, with and without BTP2. **B**, Example line scans from myocytes paced at 1Hz. Arrowheads indicate sparks occurring during diastole (n=4 animals each group, 30–40 myocytes). (**p* 0.05, ***p* 0.01)

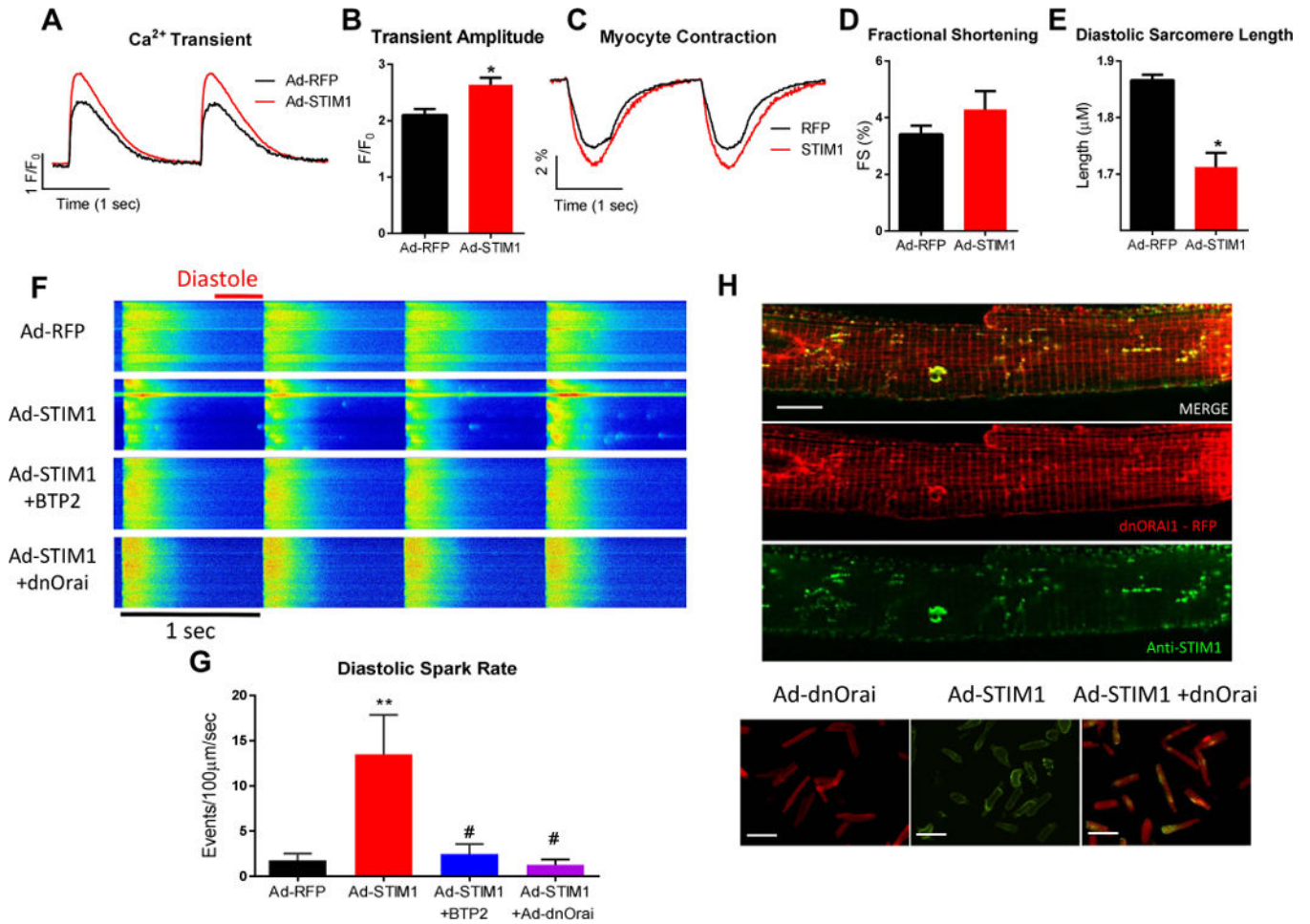


Figure 5. STIM1 Expression in Cultured AFMs Causes Diastolic Ca²⁺ Sparks by Associating with Orai Channels

A, Example trace of Ca²⁺ transients in control or STIM1 expressing myocytes. **B**, Ca²⁺ transient amplitude. **C**, Example cell shortening trace as measured by sarcomere length. **D**, Fractional shortening of myocyte contractions. **E**, Average sarcomere length during diastole when paced. **F**, Line scans from myocytes paced at 1Hz. Myocytes were infected with Ad-RFP or Ad-STIM1 and incubated with 1 µM BTP2 or co-infected with Ad-dnOrai. **G**, Spark rates during the diastolic period in myocytes from **G** (n=21–32 myocytes). **H**, *Top*: Cultured AFMs expressing both STIM1 and dnOrai have an overlapping staining pattern. *Scale bar* = 15 µm. *Bottom*: Example images of myocytes overexpressing dnOrai, STIM1, or both, demonstrating adenovirus expression in all myocytes. *Scale bar* = 50 µm. (**p* 0.05 vs. Ad-RFP, ***p* 0.01 vs Ad-RFP, #*p* 0.05 vs Ad-STIM1)

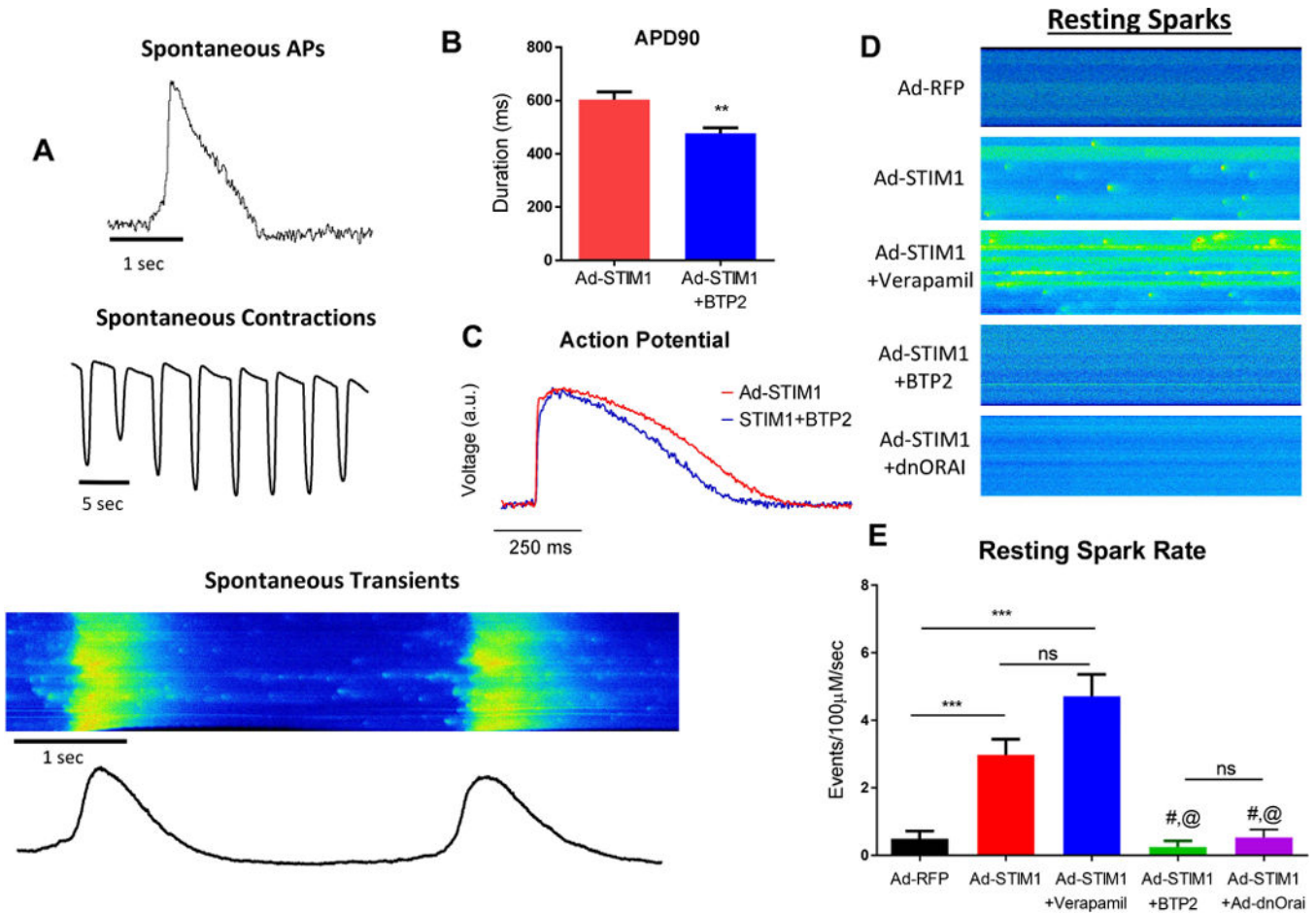


Figure 6. STIM1 Causes Spontaneous APs by Increasing Ca²⁺ Spark Rate

A, Top: di-8-anneps fluorescence recording of a spontaneously contracting, STIM1 expressing myocyte. **Middle:** Contraction traces from a spontaneously contracting, STIM1 expressing myocyte. **Bottom:** Line scan of Ca²⁺ sparks and transients with corresponding fluorescence intensity trace from a spontaneously contracting, STIM1 expressing myocyte. **B,** Time from stimulus to 90% repolarization from peak (APD90) of STIM1 expressing cells, with (n=15) and without BTP2 (n=14). **C,** Example trace of APs recorded with di-8-anneps. **D,** Line Scans of unpaced myocytes with Ad-RFP or Ad-STIM1, with verapamil, BTP2, or Ad-dnOrai co-expression. **E,** Quantitated spark rates of unpaced myocytes from D (n=15–20 myocytes). (**p 0.01, ***p 0.001, #p 0.01 vs, Ad-STIM1, @p 0.01 vs, Ad-STIM1 + Verapamil)

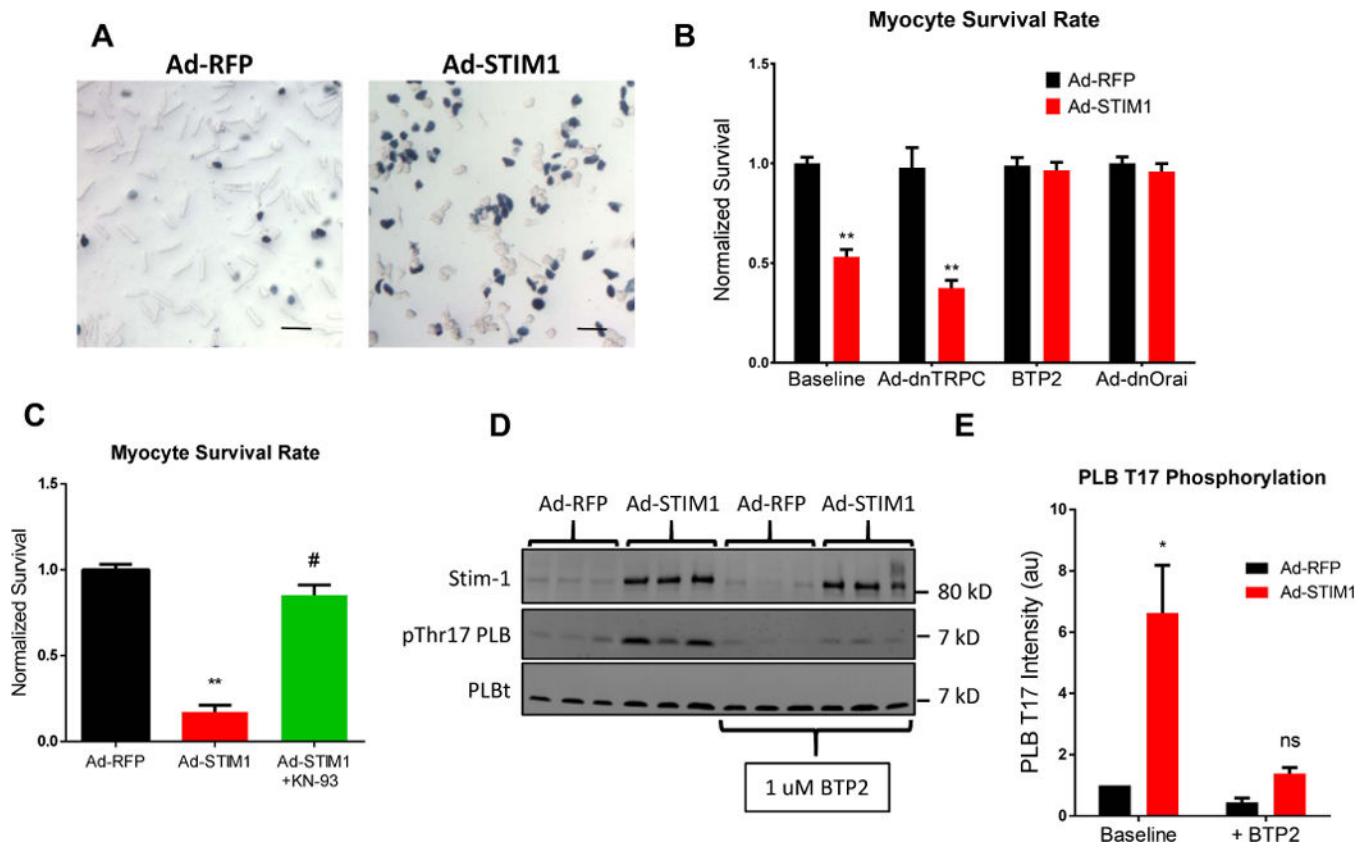


Figure 7. STIM1-Orai Mediated Ca^{2+} Influx Activates CaMKII and Causes Cell Death
A, Representative images of myocytes with RFP or STIM1 expression after 72 hours, stained with trypan blue. **B**, Myocyte viability assessed by trypan blue exclusion (n=3 separate experiments, with 6 plates each group). *Scale bar = 100 μ m* **C**, Western blot of STIM1 expression, PLB phosphorylation at Thr-17, and total PLB in RFP or STIM1 expressing myocytes after pacing at 1 Hz for 30 minutes. Myocytes were also incubated with BTP2. **D**, Quantification of PLB Thr-17 phosphorylation normalized to total PLB. **E**, Myocyte viability assessed by trypan blue exclusion. (**p* 0.05 vs. Ad-RFP, ***p* 0.01 vs Ad-RFP, #*p* 0.01 vs Ad-STIM1)